

# VU Research Portal

## Enzymatic Activity and Excited State Processes in Protochlorophyllide Oxidoreductase

Sytina, O.

2010

### **document version**

Publisher's PDF, also known as Version of record

[Link to publication in VU Research Portal](#)

### **citation for published version (APA)**

Sytina, O. (2010). *Enzymatic Activity and Excited State Processes in Protochlorophyllide Oxidoreductase*.

### **General rights**

Copyright and moral rights for the publications made accessible in the public portal are retained by the authors and/or other copyright owners and it is a condition of accessing publications that users recognise and abide by the legal requirements associated with these rights.

- Users may download and print one copy of any publication from the public portal for the purpose of private study or research.
- You may not further distribute the material or use it for any profit-making activity or commercial gain
- You may freely distribute the URL identifying the publication in the public portal ?

### **Take down policy**

If you believe that this document breaches copyright please contact us providing details, and we will remove access to the work immediately and investigate your claim.

### **E-mail address:**

[vuresearchportal.ub@vu.nl](mailto:vuresearchportal.ub@vu.nl)

## ~ CHAPTER 4 ~

**Vibrational Spectroscopy of the POR:Pchlide:NADPH Complex**

Olga A. Sytina, Maxime T. Alexandre, Bruno Robert, Rienk van Grondelle and Marie Louise Groot

In the preceding chapters the formation of the catalytic intermediate I675\* was shown to occur only after the Pchlide substrate has cycled through the excited state at least once. This remarkable effect may arise from a more favorable catalytic configuration of the enzyme-substrate complex, induced upon absorption of the first photon. Subsequently recorded absorption difference spectra in the mid-infrared region, as a function of photon flux, indeed showed two distinct phases in spectral evolution, indicating that the enzyme undergoes two separate processes upon illumination. In this chapter the results from several spectroscopic studies characterizing the Pchlide vibrational frequencies are presented, in order to provide a reliable interpretation of the mid-IR difference spectra associated with these two phases. The results presented here provide support for the assignment made earlier. The protein spectral changes seem to involve both  $\alpha$ -helix and  $\beta$ -strands domains, activation of the enzyme may therefore involve structural changes in the Rossmann folds of POR, that binds the NADPH cofactor. The  $^{13}\text{C}=\text{O}$  keto of Pchlide in the protein has a relatively low vibrational frequency of  $1653\text{ cm}^{-1}$ , which indicates that binding of Pchlide results in a very strong hydrogen bond between the keto group and a protein residue. The position of the  $\text{C}=\text{C}$  vibrational frequencies suggests a five-coordinated state of Pchlide in POR, and consequently a coordination interaction between the Pchlide Mg atom and protein residues, or water molecule. We further tentatively conclude that the formation of the I675\* catalytic intermediate is associated in the mid-IR region with decrease of the  $\text{C}=\text{O}$  keto oscillator strength.

## 4.1. Introduction

We demonstrated in chapter 2 and 3, by means of ultrafast visible transient absorption spectroscopy and fitting the TA data with a branched kinetic scheme, that in the POR enzyme the reactions of proton and hydride transfer are enabled after the substrate has cycled through the excited state at least once. We suggested that this remarkable effect may arise from a more favorable catalytic configuration of the enzyme-substrate complex, caused by conformational changes in the active site. The changes in electron distribution in the excited state of the substrate Pchlide or formation of the Pchlide triplet state may serve as trigger for this protein conformational rearrangement. The chemical structure of Pchlide is depicted in figure 4.1.

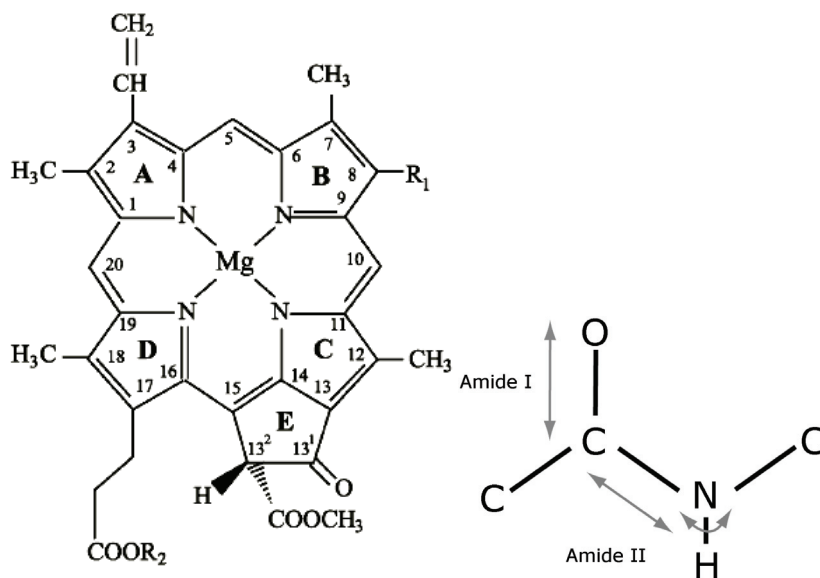


**Figure 4.1.** Chemical structure of Pchlide and protein peptide group (right).

Infrared spectroscopy is a proven tool to detect structural changes in pigment-protein molecular systems caused by light absorption or a reaction<sup>(42, 62-64)</sup>. Therefore, we performed measurements on the POR:Pchlide:NADPH complex using the rapid-scan FTIR technique, briefly described in chapter 2. As shown there, the FTIR data indeed confirmed that the protein undergoes a conformational change before photoreduction of Pchlide. Protein motions had already been shown to be important for the catalytic mechanism of

POR during the release of the formed product<sup>(17-19)</sup>. In general, the successful performance of enzymes requires the switching between different states: first a substrate and possibly a cofactor need to be bound; then the actual catalytic reaction is performed; and then the products need to be released. Each of these states may involve specific conformations. The stimulus for enzyme dynamics can be substrate binding itself, or/and allosteric binding at an additional site. Chemical and physical factors of the environment, such as pH and temperature also affect enzyme's functioning. Several enzymes have been reported to have a rest configuration and an active configuration and the dynamic interconversion between such different conformational states is important for catalysis<sup>(25-27)</sup>. The results of chapter 2 showed that in POR conformational changes are required to activate the enzyme, and that these changes are initiated by light absorption.

The photon flux- and time-dependent FTIR difference spectra as reported in chapter 2, revealed numerous bands and complex dynamics, with at least two distinct phases. A brief analysis and assignment of bands was presented in chapter 2. In this chapter, we present the full collection of datasets, recorded under different illumination conditions. The assignment of the differential signals of the POR complex requires accounting the contributions from dark and light states of all chemical species. Negative bands in the FTIR difference absorption spectrum arise from disappearance of IR absorptions associated with Pchl<sub>a</sub>, NADPH and POR enzyme in the dark state, and positive bands may arise from the appearance of new species upon illumination: Chl<sub>a</sub>, NADP<sup>+</sup> and light-activated POR. Each species has strong infrared-active modes in the 1800-1250 cm<sup>-1</sup> spectral region, what makes interpreting the spectra quite intricate and complex. For the protein, these are the N-H, C=O, and C-C vibrations of the peptide groups, composing the amide I and II bands. Pchl<sub>a</sub>, Chl<sub>a</sub> and NADPH contain C=O, C=C, C-C, and C-H groups in this spectral region; and also the tyrosine – a proton donating residue of POR has modes in this region that are expected to produce a difference signal upon proton transfer.

To obtain a more reliable assignment of the FTIR difference spectra, we carried out Fluorescence Line Narrowing (FLN) experiments on the POR complex. FLN is an ideal technique to sort out vibrational modes of the bound substrate from the overlapping protein signals, since only the substrate and not the protein will contribute to the fluorescent signal. FLN spectroscopy is performed at low temperature to eliminate the effects of spectral diffusion and thermal line broadening and to allow the observation of the vibrationally resolved emission spectrum of chromophores<sup>(65, 66)</sup>. In solution or in amorphous matrices, all chromophore molecules experience a different local environment and therefore the absorption and emission lines are broadened. If one excites a chromophore with a narrow laser pulse, spectrally matching the red-most S<sub>0</sub>-S<sub>1</sub> energy gap, then a set of emissions

corresponding to transitions from the lowest vibrational level of the S1 to all allowed vibrational levels on the S0 can be detected, using a CCD camera. The energy difference between the excitation pulse and emissions corresponds to the vibrational energies of the ground state.

In our FLN measurements the excitation wavelength was set at 647.1 nm to selectively excite a subset of bound pigments with the lowest energy S0–S1 transition. For the unbound Pchl<sub>a</sub> the maximum of the Q<sub>y</sub> absorption band is located at 630 nm, and for the bound state it red-shifts to 640 nm. The first reaction intermediate in the POR photoreaction appears at temperatures above 120 K<sup>(5, 19)</sup>, thus selective excitation of the bound Pchl<sub>a</sub> at 647.1 nm at lower temperatures (10 K) traps the reaction and does not photoconvert substrate into intermediate and final products. In this way the vibrational modes of the POR-bound Pchl<sub>a</sub> chromophore could be resolved.

We further present the results of mid-IR transient absorption measurements on the POR complex, carried out to investigate the Pchl<sub>a</sub> dynamics at RT over a 3 ns time range after excitation. In the Appendix to this chapter, Resonance Raman and FTIR spectra of isolated Pchl<sub>a</sub> in solution are presented to illustrate the positions of its vibrational modes in monomer and aggregated states.

## 4.2. Materials and Methods

POR:Pchl<sub>a</sub>:NADPH samples at concentrations of 0.5 mM thermophilic POR, 0.5 mM Pchl<sub>a</sub> and 3.5 mM NADPH in D<sub>2</sub>O, and H<sub>2</sub>O Tris/Triton buffer solutions were used in the FLN and FTIR experiments. The samples were stored in the dark prior to all measurements to ensure absence of any light-induced catalytic products.

The FLN spectrum was recorded using a U1000 double monochromator (Jobin Yvon, Longjumeau, France) equipped with an ultra-sensitive, deep-depleted, front illuminated CCD (Jobin Yvon). Excitation at 647.1 nm was provided by an Innova 100 argon laser (Coherent, Palo Alto, California). The spectra were obtained at a spectral resolution of 1 cm<sup>-1</sup>. During measurements, the samples were kept at 10 K in a helium flow cryostat (Air Liquide, Sassenage, France). The laser power was less than 100 μW.

Light-minus-dark difference spectra were recorded by means of an FTIR Bruker IFS 66/S spectrometer in rapid-scan mode. The excitation laser beam covered the major area of the 20 μm thick sample cell, and the excitation intensity was adjusted to the intensity used in the visible pump-probe measurements to less than 0.5 mJ/cm<sup>2</sup>.

Transient visible pump mid-IR probe spectra of the POR complex were recorded using the setup described in Groot *et al.*<sup>(64, 67)</sup>. The POR complex was excited at 475 nm,

using a 20  $\mu\text{m}$  thick sample cell. The concentration was two times higher than for the FLN and FTIR measurements.

### 4.3. Results

#### 4.3.1. Fluorescence Line Narrowing Spectroscopy

The FLN spectra of the POR:Pchlide:NADPH complex recorded in  $\text{H}_2\text{O}$  and  $\text{D}_2\text{O}$  Tris/Triton buffered solutions, at 10 K and using 647.1 nm excitation are shown in figure 4.2. For control we recorded the FLN spectrum of Pchlide dissolved in methanol under the same conditions.

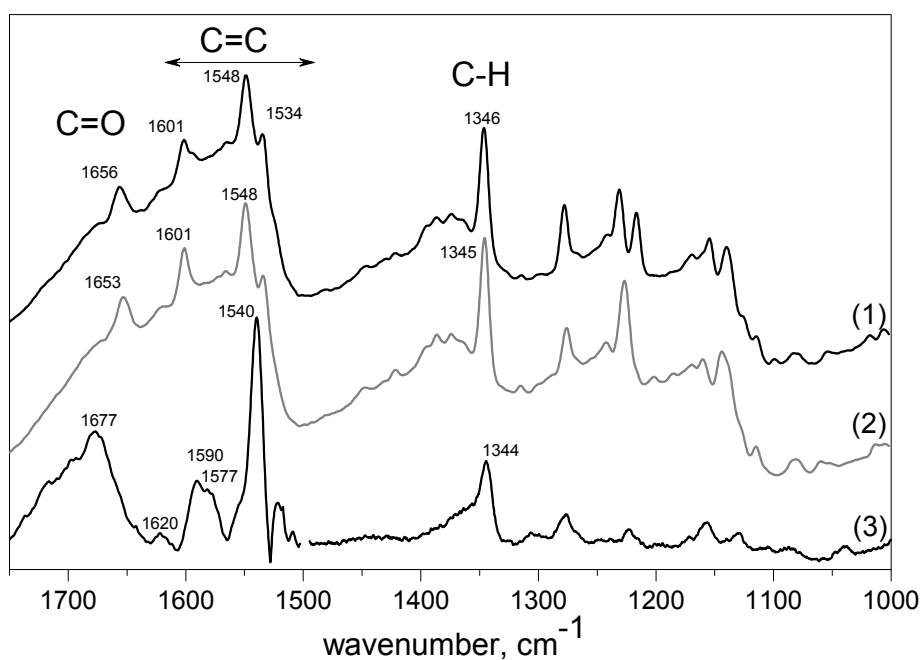


**Figure 4.2.** FLN spectrum of POR-bound Pchlide recorded at 10K upon 647.1 nm excitation in  $\text{H}_2\text{O}$  buffer (1),  $\text{D}_2\text{O}$  buffer (2), and free Pchlide in methanol (3). The spectral resolution is better than 1  $\text{cm}^{-1}$ .

The spectra of POR-bound Pchl<sub>a</sub> in H<sub>2</sub>O (black line) and D<sub>2</sub>O (red line) are very similar to each other, except that the positions of several bands are slightly shifted, consistent with an isotope effect. The spectrum of Pchl<sub>a</sub> dissolved in methanol shows more extensive shifts of the vibrational modes. In the unbound state in methanol, major bands are located at 1677 cm<sup>-1</sup>, 1620 cm<sup>-1</sup>, a double peaked band at 1590/1578 cm<sup>-1</sup>, and 1540 cm<sup>-1</sup>. In the POR-bound state the 1677 cm<sup>-1</sup> band is downshifted to 1656 cm<sup>-1</sup> in H<sub>2</sub>O and to 1653 cm<sup>-1</sup> in D<sub>2</sub>O; the 1620 cm<sup>-1</sup> band is unchanged; the band at 1590/1578 cm<sup>-1</sup> is upshifted to 1601 cm<sup>-1</sup>, and instead of the single 1540 cm<sup>-1</sup> band there are two bands at 1548 cm<sup>-1</sup> and 1534 cm<sup>-1</sup>. At lower frequencies, in the H<sub>2</sub>O and D<sub>2</sub>O spectra we can see relatively weak and broad signals between 1450 cm<sup>-1</sup> and 1375 cm<sup>-1</sup>, and intense bands at 1346 cm<sup>-1</sup> and 1345 cm<sup>-1</sup>. The intense bands below 1275 cm<sup>-1</sup> do not overlap with the spectral window of our FTIR experiment, and therefore will not be further discussed in this work.

#### **4.3.2. Variation of difference absorption FTIR spectra**

We used FTIR absorption difference spectroscopy in order to investigate whether conformational changes in the POR enzyme are induced upon absorption of a photon. The difference spectra (light-minus-dark) were recorded every second using the FTIR apparatus in rapid-scan mode, while flashing with 5-ns laser pulses at a 20 Hz repetition rate to excite the enzyme-substrate complex. The data from continued flashing and stopped flashing experiments have been discussed in chapter 2, these data are reproduced here in figure 4.3 A, B. We additionally present results from measurements recorded under slightly different conditions, shown in figure 4.3.C, D.

Figure 4.3.A shows evolution-associated difference spectra resulting from a global sequential kinetic analysis of FTIR light-minus-dark difference spectra, collected every second. In this experiment the pump laser was turned off after 5 seconds whereas spectra were collected during 30 seconds. The time/photon flux dependent behavior of the data can be described with a sequential model A→B→C→, with increasing lifetimes/photon fluxes  $\tau_1$ ,  $\tau_2$ ,  $\tau_3$ . The final blue spectrum has an (on the time scale of the experiment) infinite lifetime. In the next experiment (figure 4.3.B), illumination was continued during 60 s which resulted in a significantly different spectrum (blue) after ~60 s (or ~1200 laser pulses).

The data depicted in figure 4.3.C were recorded using the same excitation conditions as for the continued flashing experiments (444 nm at 20 Hz), but the spectra were recorded every 10 seconds instead of every 1 second, and with a higher spectral resolution of 4 cm<sup>-1</sup>. The initial spectrum in the -1654 cm<sup>-1</sup>/+1643-1633 cm<sup>-1</sup> region (black line in figure 4.3.C)

is very similar to the initial phase resolved in previous two measurements (compare dashed line in figure 4.3.C). Then it evolves into the spectrum similar to the final blue state in figure 4.3.B with the characteristic  $-1570/+1450\text{ cm}^{-1}$  bandshift. The  $+1540\text{ cm}^{-1}$  amide II band is more intense and there is no gain in its amplitude during 30 seconds.

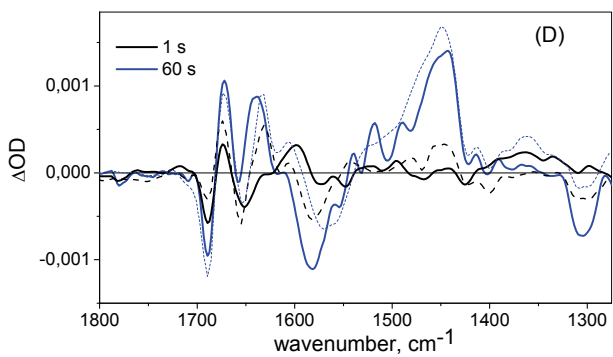
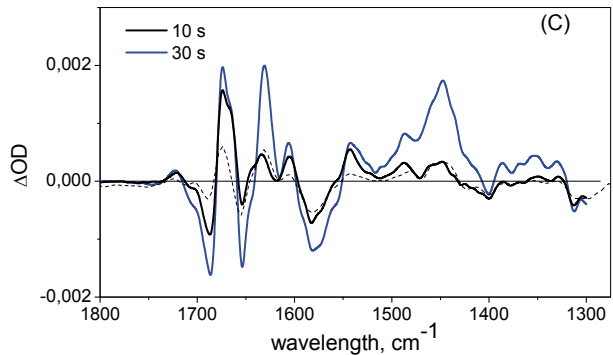
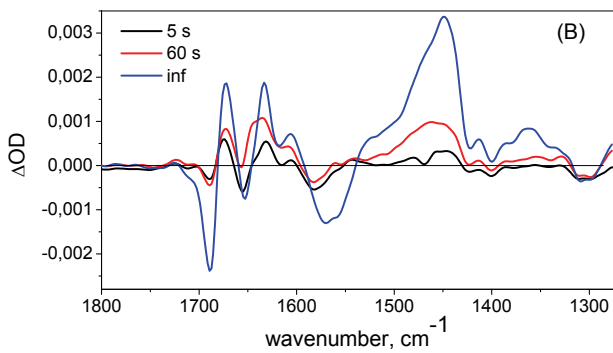
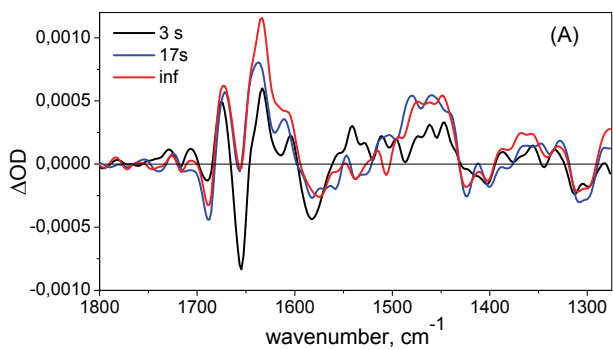
Usually the main source of noise in FTIR experiments in the  $1800\text{--}1200\text{ cm}^{-1}$  spectral region is water vapor absorption. The water lines are much sharper than differential signals of the POR complex. Therefore the choice for a lower resolution (figure 4.3.A, B) allowed us to eliminate the contribution of a fluctuating baseline to an acceptable level. Also the movable mirror in the interferometer is running at a frequency of 100 kHz, and therefore the choice of lower spectral resolution of  $8\text{ cm}^{-1}$ , and a consequently shorter distance for the moving mirror, allows more scans to be acquired during the same period of time, as compared to the  $4\text{ cm}^{-1}$  resolution settings.

We also tested the 475 nm LED illumination, instead of laser illumination, in another series of rapid-scan FTIR measurements on the POR:Pchl $_{a}$ :NADPH samples (figure 4.3.D). Despite the fact that the photon flux was less controlled, two distinct phases are clearly resolved after 1 second and 60 seconds of continuous illumination. The result of this experiment is similar to the 5 s and infinite spectra obtained from the global analysis of the continued-flashing laser experiment (compare dashed lines in figure 4.3.D).

Despite some variation in the obtained spectra, consistently at least two distinct phases in the time-resolved infrared dynamics can be distinguished, with the later only appearing upon continued illumination. We associated the initial process mainly with protein conformational dynamics, and the later phase with mainly formation of catalytic product<sup>(52)</sup>, we will return to this assignment in the discussion.

**Figure 4.3.** next page **(A)** EADS of the stopped-flashing experiment. The illumination was on for 5 s, acquisition time was 30 s,  $8\text{ cm}^{-1}$  spectral resolution. **(B)** EADS of the continued-flashing experiment. Illumination was on during the acquisition time of 60 s,  $8\text{ cm}^{-1}$  spectral resolution. **(C)** Time-gated light-minus-dark difference spectra recorded after 10 s and 30 s of laser illumination,  $4\text{ cm}^{-1}$  spectral resolution. Dashed black line corresponds to the 5 s spectrum from panel B. **(D)** Time-gated light-minus-dark difference spectra recorded after 1 s of 475 nm LED illumination (black) and after 60 s of LED illumination (blue),  $8\text{ cm}^{-1}$  spectral resolution. Dashed black line corresponds to the 5 s spectrum from panel B, dashed blue is the inf spectrum from panel B.





### 4.3.3. Mid-IR transient absorption spectroscopy

In contrast to the relatively slow protein dynamics resolved in the FTIR difference absorption experiment, in this section the main focus will be on the ultrafast dynamics in the POR complex measured in the 1800-1590  $\text{cm}^{-1}$  spectral region, over a -15 ps to 3000 ps time range. The mid-IR time-resolved data was analyzed with a global algorithm using four sequentially decaying exponential components with increasing lifetimes. The evolution-associated difference spectra (EADS) are shown in figure 4.4. Because of the lower signal to noise level in these experiments, the presented dataset consists of 20 individual sample scans averaged together. This means that the effect of a first and second and subsequent photon can not be distinguished and that these data can be compared with the results obtained in the visible only qualitatively.

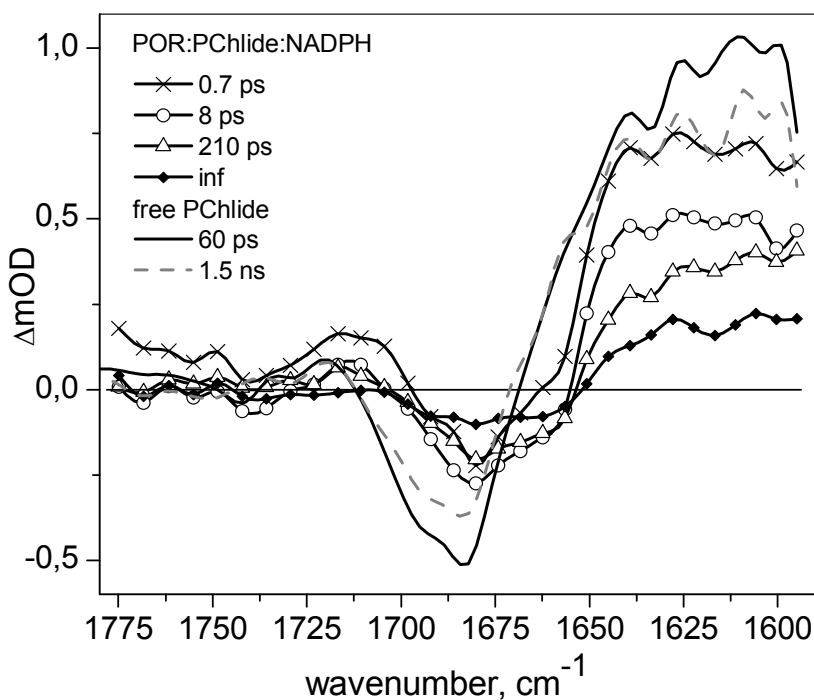


**Figure 4.4.** EADS resulted from global analysis of a dataset consisted of 20 consecutive scans of POR sample in  $\text{D}_2\text{O}$  Tris/Triton buffer solution pumped at 475 nm (solid lines). EADS of free Pchlride in  $\text{D}_2\text{O}$  Tris/Triton buffer pumped at 475 nm (dashed lines).

Negative bands at  $1735\text{ cm}^{-1}$  and between  $1700$  and  $1650\text{ cm}^{-1}$  correspond to ground state bleaching of the ester and keto modes respectively. The negative signal around  $1680\text{ cm}^{-1}$  seems to be composed of three bands at  $1690\text{ cm}^{-1}$ ,  $1680\text{ cm}^{-1}$  and  $1658\text{ cm}^{-1}$ . A broad structureless positive signal, originating from the keto group in the electronic excited state is observed at  $1650$ - $1590\text{ cm}^{-1}$  and a relatively weak positive signal is also present at  $1725$ - $1700\text{ cm}^{-1}$ . The TA spectra of free Pchl $\text{id}$ e in  $\text{D}_2\text{O}$  buffered solution is overlaid in figure 4.4 for reference. It shows a double peaked negative band with maxima at  $1695\text{ cm}^{-1}$  and  $1682\text{ cm}^{-1}$ , and a positive signal with fine structure, similar to that in the POR spectrum, extends down to  $1590\text{ cm}^{-1}$ . The POR:Pchl $\text{id}$ e:NADPH complex shows more dynamics than free Pchl $\text{id}$ e in  $\text{D}_2\text{O}$  buffer. With time constants similar to those observed in the visible spectral region (see table 3.1 in chapter 3) a decay of intensity of the positive absorption due to the keto in the excited state occurs, concurrent with a decay of the bleaching intensity.

#### 4.4. Discussion

In the following section we discuss the IR data and present a refined assignment of the bands in the FTIR data from chapter 2 (and figure 4.3.B).

##### 4.4.1. Assignment of bands in FLN spectrum

The FLN spectroscopy allowed us to detect vibrational modes in the ground state of Pchl $\text{id}$ e bound to the enzyme. The understanding of the FLN data will help to determine which negative bands in the FTIR spectrum belong to POR-bound Pchl $\text{id}$ e.

The Pchl $\text{id}$ e molecule has one keto  $\text{C}=\text{O}$  group in the  $13^1$  position which is the strongest infrared marker in the high-frequency spectral region. The typical position for the  $\text{C}=\text{O}$  keto band in chlorophylls is usually found in the  $1700$ - $1650\text{ cm}^{-1}$  spectral region, depending on coordination and H-bonding interactions between chromophore and solvent or protein. For example, in Chl  $a$  in THF the ester  $\text{C}=\text{O}$  mode appears around  $1740\text{ cm}^{-1}$  and the keto  $\text{C}13=\text{O}$  between  $1698/1660\text{ cm}^{-1}$  in the ground state<sup>(67, 68)</sup>. From the mid-IR TA measurements on Pchl $\text{id}$ e in different solvents, presented in chapters 5 and 6, it is inferred that H-bonding interaction significantly downshifts the position of the keto group from  $1708\text{ cm}^{-1}$  in the aprotic solvent THF to a set of modes varying between  $1700\text{ cm}^{-1}$  and  $1650\text{ cm}^{-1}$  in the protic solvents such as methanol,  $\text{D}_2\text{O}$  Tris/Triton buffer and neat  $\text{D}_2\text{O}$ . Hence, we conclude that the strong  $1677\text{ cm}^{-1}$  band of Pchl $\text{id}$ e in methanol in the FLN spectrum belongs to the keto  $\text{C}=\text{O}$  mode. We further conclude from the FLN measurements that in the POR protein, the keto frequency is at  $1653\text{ cm}^{-1}$  in  $\text{D}_2\text{O}$ , and at

1656  $\text{cm}^{-1}$  in  $\text{H}_2\text{O}$ . These low frequencies indicate a very strong hydrogen bond of the Pchlido keto group to a protein residue in the POR active site. The 3  $\text{cm}^{-1}$  difference in the C=O frequencies of bound Pchlido in  $\text{H}_2\text{O}$  and in  $\text{D}_2\text{O}$  is in good agreement with an H/D substitution shift of protein residuals inside the binding site<sup>(69)</sup>. Though the  $^{13}\text{C}$  C=O keto on the E ring of Pchlido does not participate directly in proton and hydride transfer in the catalytic reaction, any structural alterations in the E ring were shown to disrupt Pchlido's ability to act as a substrate<sup>(7)</sup>. Also, the E and D rings are considered to be fixed at the Rossman fold of POR, which represents its active site<sup>(4)</sup>.

The intense bands in both methanol and the POR complex in the lower region down to 1500  $\text{cm}^{-1}$  are likely to be due to the C=C vibrations, typically located in this region in Chl and Bchl<sup>(45, 70-73)</sup>. Previously, the bands between 1570  $\text{cm}^{-1}$  and 1400  $\text{cm}^{-1}$  in the infrared spectrum of Bchl and pheophytine were attributed either to C=C or C-C stretching modes<sup>(44, 45)</sup>. Weak bands at 1612-1606  $\text{cm}^{-1}$  and strong bands between 1550-1530  $\text{cm}^{-1}$  in Chl and Bchl were assigned to the C=C double bond vibrations<sup>(44, 45, 70, 71)</sup>. The C=C vibrational frequencies are sensitive to the coordination number of the central Mg atom. In Chl and Bchl the change in the coordination number in different solvents going from 5 (one axial ligands) to 6 (two axial ligands) is accompanied by a downshift in the C=C vibrational frequencies from 1612/1606  $\text{cm}^{-1}$  to 1599/1595  $\text{cm}^{-1}$  respectively; the 1554/1551  $\text{cm}^{-1}$  modes downshift to 1548/1545  $\text{cm}^{-1}$ ; the 1529/1527  $\text{cm}^{-1}$  modes shift to 1521/1518  $\text{cm}^{-1}$ <sup>(70, 71)</sup>. The FLN bands in this region for Pchlido in methanol and POR-bound Pchlido are located at 1590  $\text{cm}^{-1}$  and 1601  $\text{cm}^{-1}$ , respectively. Since Pchlido in methanol can be assumed to be six-coordinated<sup>(70, 72, 74)</sup>, it appears that in the protein, Pchlido is in the five-coordinated state.

The C-C single bond is expected at a lower frequency than the C=C modes because of the lower bond force constant, corresponding to a weakening/loosening of vibrations. Normal mode analysis assigns intense bands at 1470-1430  $\text{cm}^{-1}$ , observed in the infrared spectrum of ethyl-chlorophyllide, to 22 skeletal vibrations<sup>(75)</sup>. Therefore we conclude that the group of less intense bands between 1450-1375  $\text{cm}^{-1}$  very likely belongs to C-C skeletal vibrations. The positions of the skeletal C=C and C-C modes of bound Pchlido remain unchanged upon H/D substitution, which indicates that the macrocyclic structure of Pchlido is not involved in H-bonding interaction with the POR enzyme.

Additional measurements (ATR FTIR, Raman) on Pchlido in different solvents are described in the Appendix to this chapter. Consistent with the assignment given here, a number of intense Raman C=C bands in the region 1600-1500  $\text{cm}^{-1}$  are resolved for Pchlido in different solvents, and bands between 1470-1430  $\text{cm}^{-1}$  are weaker in intensity.

The C–H stretching vibrations in the infrared absorption spectrum of BChl were assigned to the 1380-1320  $\text{cm}^{-1}$  region<sup>(44)</sup>. In the Raman spectrum of Chl d<sup>(76)</sup>, the C17–H and C18–H in plane bending modes were observed at 1309  $\text{cm}^{-1}$ , with calculated values at 1319  $\text{cm}^{-1}$ . Therefore, most likely, the intense 1346/1345  $\text{cm}^{-1}$  band belongs to C–H/C–D stretching modes respectively. The small downshift in the vibrational frequency with POR bound Pchlde in either H<sub>2</sub>O or D<sub>2</sub>O again indicates that interaction with protein residues is involved.

#### 4.4.2. Assignment of bands in FTIR spectrum

##### 1700-1600 $\text{cm}^{-1}$ region

The continued flashing FTIR difference spectra together with the steady-state absorption spectrum of the POR complex are plotted in one graph (figure 4.5). The 1700-1600  $\text{cm}^{-1}$  region in the difference spectra is the most crowded and demonstrates complex dynamics. The contributions from the C=O keto modes of both cofactor NADPH and Pchlde in the ground state are expected, in the light-induced state, because of the formation of NADP<sup>+</sup> and Chlide, modes can shift in frequency and additionally there might be protein amide I band signals.

In the steady-state spectrum (green line in figure 4.5) we find three distinct and broad bands at 1644  $\text{cm}^{-1}$ , 1570-1550  $\text{cm}^{-1}$  and 1458-1460  $\text{cm}^{-1}$ . The vibrational modes of Pchlde and NADPH are not resolved. Clearly, the positive signals at 1640  $\text{cm}^{-1}$  and 1630  $\text{cm}^{-1}$  in the black and red difference spectra are reproducing the shape of the amide I band in the steady-state regime. The amide I is the most intense absorption band in proteins originating from C=O stretching vibrations of peptide groups (figure 4.1) with a minor contribution of C–N stretching. The frequencies are determined by the secondary structure, i.e. the backbone conformations and the H-bonding pattern. Typically, the amide I band position in proteins ranges from 1700  $\text{cm}^{-1}$  to 1600  $\text{cm}^{-1}$  and is a convolution of multiple components<sup>(77)</sup>. The average position of the  $\alpha$ -helix characteristic frequency is around 1660-1645  $\text{cm}^{-1}$ , dual bands at 1640-1620  $\text{cm}^{-1}$  and 1689-1682  $\text{cm}^{-1}$  belong to  $\beta$ -strands, and turns are usually located at 1682-1662  $\text{cm}^{-1}$ , whereas the  $\alpha$ -helix in D<sub>2</sub>O is located at 1645  $\text{cm}^{-1}$ <sup>(78)</sup>. Therefore, we conclude that the light-induced dual band in the difference initial FTIR spectrum (black, red lines in figure 4.5) at 1644-1634  $\text{cm}^{-1}$  and the negative/positive features at 1688  $\text{cm}^{-1}$  and 1675  $\text{cm}^{-1}$ , respectively can be explained by downshifts of the amide I bands of  $\alpha$ -helix and  $\beta$ -sheet structures, as a results from rearrangement in the secondary structure taking place after excitation of Pchlde. The negative band around 1580  $\text{cm}^{-1}$  is consistent with an amide II response. This shows that the initial spectral changes in

the POR complex can be assigned to protein conformational changes only. As the spectral changes seem to be concurrent in both  $\alpha$ -helix and  $\beta$ -strands domains, the changes may take place in the Rossmann fold of POR, composed of three or more parallel  $\beta$ -strands linked by two  $\alpha$ -helices in the topological order  $\beta$ - $\alpha$ - $\beta$ - $\alpha$ - $\beta$  that binds the NADPH cofactor<sup>(4, 12)</sup>. The second spectral phase is represented by the blue spectrum, which is clearly different from the earlier phase and shows negative bands at 1688  $\text{cm}^{-1}$ , 1653  $\text{cm}^{-1}$  and 1570  $\text{cm}^{-1}$ , and positive bands at 1673  $\text{cm}^{-1}$ , 1630  $\text{cm}^{-1}$ , 1450  $\text{cm}^{-1}$  and 1361  $\text{cm}^{-1}$ .

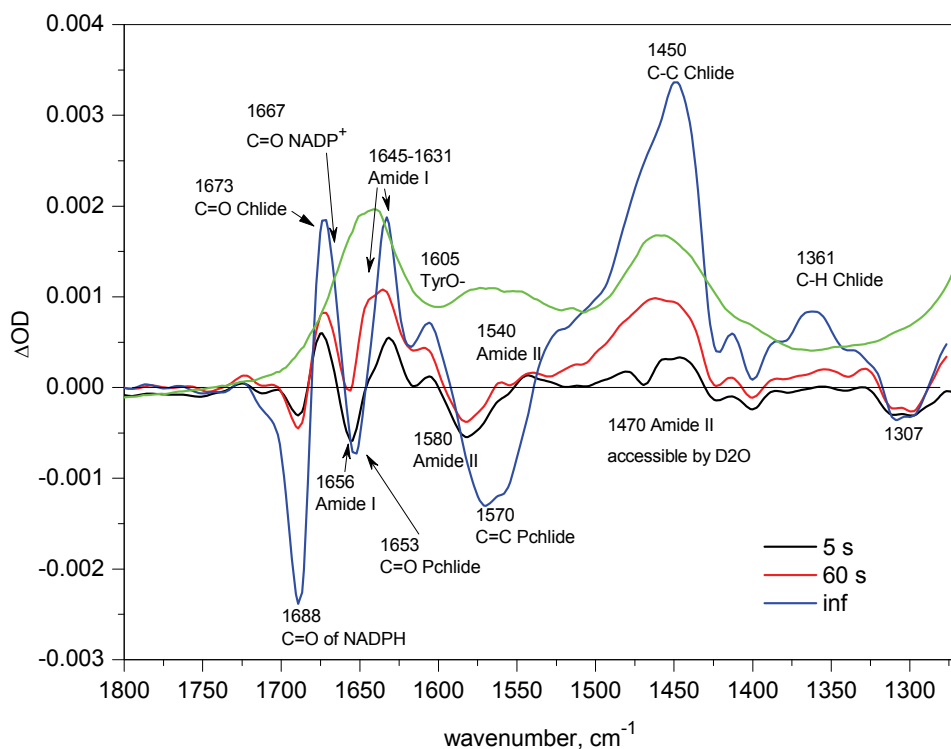


**Figure 4.5.** FTIR difference absorption spectra (black, red, blue) and steady-state absorption of the POR complex (green line) with the assignment of main bands.

Free NADPH dissolved in  $\text{D}_2\text{O}$  buffered solution has a strong IR absorption due to its C=O group of the nicotine amide ring at 1688  $\text{cm}^{-1}$ , which in  $\text{NADP}^+$  downshifts to 1667  $\text{cm}^{-1}$  (43, 79). Whether the frequency of the keto C=O stretching in NADPH experiences

any downshift when bound in the active site of POR depends on its involvement into H-bonding interaction with protein residues. According to Iwaki, and Jackson<sup>(43)</sup>, NADPH when bound to transhydrogenase enzyme demonstrates a signal of the keto group at a slightly lower frequency, at  $1684\text{ cm}^{-1}$ . Thus, the most obvious assignment of the negative signal at  $1687\text{ cm}^{-1}$  in our FTIR spectrum is the bleach of the NADPH keto, due to hydride transfer. Where we expect a positive band from  $\text{NADP}^+$ , we find a peak at  $1673\text{ cm}^{-1}$ . In the FTIR experiment, with  $4\text{ cm}^{-1}$  spectral resolution (figure 4.3.C), a shoulder in this band is resolved, peaking at  $1667\text{ cm}^{-1}$  band. Therefore the  $\text{NADP}^+$  can be safely assigned to either of these two signals. Also in this region we could expect the contribution from the C=O of newly formed Chlide. The position of Chlide C=O could not be directly determined in our experiments and can be assigned only by analogy to other chlorophyll like molecules, to the same  $1700\text{-}1650\text{ cm}^{-1}$  region. In principle we can assume that the C=O frequency of Chlide should upshift upon product release into solvent, because of weakening of H-bonding interaction around the keto. Thus, it is reasonable to assign either the main band at  $1673\text{ cm}^{-1}$  or the shoulder at  $1667\text{ cm}^{-1}$  to the C=O of Chlide. In future experiments, the positions of the Chlide C=O keto, and C=C and C-C skeletal modes can be identified more precisely using the FLN technique with selective excitation at  $670\text{-}680\text{ nm}$ , similarly to the presented measurements on POR-bound Pchl<sub>a</sub>.

From the results obtained in the FLN experiment we conclude that the negative signals at  $1653\text{ cm}^{-1}$  in the FTIR spectra can be assigned in the later stage to disappearance of bound Pchl<sub>a</sub> due to its conversion into Chlide. In the initial spectrum (black line figure 4.5) the ground state bleaching at  $1656\text{ cm}^{-1}$  evolves into the  $1653\text{ cm}^{-1}$  bleach in the next evolutions. The downshift in frequency can be considered to be the result of domination of Pchl<sub>a</sub> conversion in the later phase, whereas in the initial phase the signal originates mainly from the  $\alpha$ -helix bleach.

The Tyr-O<sup>-</sup> radical signal was found at  $1603\text{ cm}^{-1}$ <sup>(62)</sup>, which is very close to a band at  $1605\text{-}1602\text{ cm}^{-1}$  present in our FTIR difference spectra. The amplitude of this band is significantly increased upon continued illumination, when the catalytic product is supposed to dominate the difference spectra.

### **1600-1400 $\text{cm}^{-1}$ region**

The amide II is usually found in the  $1580\text{-}1510\text{ cm}^{-1}$  spectral window, and derives mainly from in plane N-H bending, C-N and C-C stretching vibrations of peptide groups<sup>(69)</sup>. The position of the amide II band is also conformational sensitive. Due to contributions of N-H stretching, a downshifted signal is expected upon substitution of protons with deuteriums at

1470-1450  $\text{cm}^{-1}$  (69, 80). Indeed, the steady-state absorption of the POR complex in this region shows two bands at 1580  $\text{cm}^{-1}$  and 1540  $\text{cm}^{-1}$ , and 1460  $\text{cm}^{-1}$ . The amide II signals overlap with the C=C skeletal modes of Pchl<sub>a</sub> and C-C modes of Chl<sub>a</sub>.

The signals at 1580  $\text{cm}^{-1}$  and 1540  $\text{cm}^{-1}$  in the first two evolutions (black, red lines in figure 4.5) are consistent with a downshift of the amide II band. It should be noted that the amplitude of this band does not increase upon continued illumination, and consequently should not be associated with proton and hydride transfer reactions. Consequently, the -1580/+1540  $\text{cm}^{-1}$  bandshift we assign to a change in amide II frequency resulting from a conformational change in the protein. The process is accompanied by changes around 1470  $\text{cm}^{-1}$  (black spectrum in figure 4.5), a region where H/D exchanged amide II peaks. Apparently not all groups in the protein are accessible for H/D exchange.

The process of Chl<sub>a</sub> accumulation can be distinguished from the protein signals only by comparison of the stopped flashing and continued flashing experiments. In the later a very intense differential signal -1570/+1450  $\text{cm}^{-1}$  appears. Using the results of the FLN experiment, we assign these signals to disappearance of the C=C double bond in Pchl<sub>a</sub> and appearance of the C-C single bond in Chl<sub>a</sub>.

### 1380-1320 $\text{cm}^{-1}$ region

The proton and hydride transfer results in the appearance of two new C-H groups in the chromophore. As can be inferred from the analysis of the FLN data, appearance of relatively intense positive signals at 1385  $\text{cm}^{-1}$ , 1360  $\text{cm}^{-1}$  and 1330  $\text{cm}^{-1}$  (blue line in figure 4.5), in the continued flashing FTIR experiment in the last evolution, can be associated with the appearance of a C-H mode.

#### 4.4.3. Ultrafast mid-IR dynamics in POR

The timescale of the mid-IR TA experiment does not overlap with the timescale of the FTIR experiment, but it does overlap with the TA measurements in the visible. However only qualitative information on the POR complex can be obtained from the mid-IR TA measurements because the consecutive sample scans need to be averaged together in order to achieve satisfactory signal to noise ratio. Therefore the information about gradual changes in the mid-IR dynamics, corresponding to the one, two and three photon processes is not available in this experiment. We applied global analysis<sup>(40)</sup> to a dataset consisting of 20 sequential sample scans to fit averaged dynamics.

In the mid-IR TA experiment we expect the dynamics of bound and unbound Pchl<sub>a</sub> and Chl<sub>a</sub> rather than protein signals, because we assume that the 3 ns time range



does not overlap with the time range of induced conformational changes in POR, registered by the FTIR method. Hence, the negative signals in the mid-IR TA spectrum originate mainly from the ground state absorption of free and POR-bound Pchl<sub>id</sub>e and Chl<sub>id</sub>e, the positive signals we expect to belong to vibrations of chromophores in the electronically excited state, and to intermediate catalytic product I675\*. A difference signal from NADPH/NADP<sup>+</sup> should not be present in this data, because according to the TA measurements on the POR:Pchl<sub>id</sub>e:NADPD complex on the micro-/millisecond timescale, hydride is transferred from NADPD with a rate of (500 ns)<sup>-1</sup> (55), which is far beyond our 3 ns range. Consistent with this, we do not see, on any time scale, bleaching of a band at 1688 cm<sup>-1</sup> or a positive absorption appearing at around 1670 cm<sup>-1</sup>, as we would expect for the hydride transfer reaction from NADPH.

The spectra show the presence of at least three bands, at 1658-1656 cm<sup>-1</sup>, ~1680 cm<sup>-1</sup> and ~1690 cm<sup>-1</sup>, suggesting that we resolve here not only the contribution from bound Pchl<sub>id</sub>e, but also from unbound Pchl<sub>id</sub>e and Chl<sub>id</sub>e. With the FLN experiments we established that the keto mode of bound Pchl<sub>id</sub>e is at 1653 cm<sup>-1</sup>. Possibly, the broad induced absorption band partially obscures the expected bleach at 1653 cm<sup>-1</sup>. Comparing with the Pchl<sub>id</sub>e in D<sub>2</sub>O spectrum, suggests in fact that this cancellation is quite effective, and that without it the 1653 cm<sup>-1</sup> band would have been the dominant negative band in the spectrum. The negative bands at ~1690 cm<sup>-1</sup> and ~1680 cm<sup>-1</sup> in the POR spectrum are similar to those in the Pchl<sub>id</sub>e in D<sub>2</sub>O spectrum, and with the 1673 cm<sup>-1</sup> frequency inferred for Chl<sub>id</sub>e. Their relatively large contribution in the TA spectra may indeed be partially due to a cancellation of the bound Pchl<sub>id</sub>e band.

Despite the overall complexity of the mid-IR TA spectrum, the distinctive feature of the excited state dynamics is a sequential decay of positive signals between 1650-1590 cm<sup>-1</sup> with rates of 0.7 ps, 8 ps and 210 ps. Free Pchl<sub>id</sub>e dissolved in Tris/Triton buffer, identical to the one used for the POR samples, does not show a downshift and decay of the positive signals to such an extent on similar timescales, see dashed lines in figure 4.4 and figure 5.5 in chapter 5. Instead, a behavior similar to that of Pchl<sub>id</sub>e in methanol and in neat D<sub>2</sub>O (discussed in more detail in chapter 5, and 6) is observed for Pchl<sub>id</sub>e in D<sub>2</sub>O buffered solution. Therefore we conclude that the dynamics in the 1650-1590 cm<sup>-1</sup> region can be associated rather with formation of the I675\* catalytic product, than with dynamics of free Pchl<sub>id</sub>e and/or Chl<sub>id</sub>e.

As we inferred previously, the I675\* catalytic intermediate is formed with ~(4 ps)<sup>-1</sup> and ~(180 ps)<sup>-1</sup> rates. Based on the KIE effect we observed for the formation of the I675\* state (in chapter 3) we associate it with proton transfer from tyrosine to the Pchl<sub>id</sub>e C18 position. The keto mode we observe here is however that at the C13 position (figure 4.1),

and tracks therefore the proton transfer event only indirectly. In addition it may be sensitive to other electronic changes accompanying or preceding the proton transfer. The proton transfer event itself will create a positive charge on the Pchl<sub>id</sub>, if it is not accompanied by a concerted electron transfer event. An indicator of a positively charged Pchl<sub>id</sub> is the presence of the positive signal around 1715 cm<sup>-1</sup>, which is usually assigned to an up shift of the keto mode upon formation of the cation state in chlorophyll-like molecules<sup>(44)</sup>. However, a small signal in this region is present in all solvents (see also dashed lines in figure 4.4), and its magnitude relative to the bleached keto band is difficult to gauge at present, because of the partial cancellation by positive signals of the unbound Pchl<sub>id</sub>. A signal from the deprotonated tyrosine signal might appear in the 1605 cm<sup>-1</sup> region. Though there are some small relative changes on the 200 ps time scale in that region, the signals are dominated by the decay of the downshifted keto band. Indeed, the oscillator strength of the tyrosine is expected to be much weaker than of the Pchl<sub>id</sub> keto. The strong decrease in intensity of the keto mode in the excited or I675\* state could be explained by weakening of the C=O dipole moment due to disappearance of some electron density or/and resulting from strengthening of H-bonding interaction. However the latter may be unlikely considering that the 1653 cm<sup>-1</sup> position is already indicative of a strong hydrogen bond. At the moment it is difficult to interpret these spectra more quantitatively than that the mid-IR TA data clearly demonstrate a correlation between formation of the first catalytic intermediate I675\* and the dynamics of the C=O keto group of Pchl<sub>id</sub>.

The two ester groups in Pchl<sub>id</sub> in the positions 13<sup>2</sup> and 17<sup>3</sup> are expected to have minor contribution to differential signals because of their remoteness from the conjugated electronic system. Typically ester modes in Pchl<sub>id</sub> are located at frequencies above 1700 cm<sup>-1</sup> (see chapter 5).

#### 4.5. Conclusions

We showed in chapter 2 and 3 that the rate and quantum yield of formation of the intermediate state I675\* is significantly enhanced after the Pchl<sub>id</sub> substrate has cycled through the excited state at least once. This remarkable effect may arise from a more favourable catalytic configuration of the enzyme-substrate complex, caused by the changed electron distribution in the Pchl<sub>id</sub> excited state. In order to investigate whether conformational changes in the enzyme are indeed induced upon the absorption of a photon, we recorded absorption difference spectra in the mid-infrared region, as a function of photon flux. The observation of two distinct phases in the mid-IR spectral evolution clearly indicates that the enzyme undergoes two separate processes upon illumination. In this chapter we have presented the results from several spectroscopic studies characterizing the

Pchlride vibrational frequencies, in order to provide a reliable interpretation of the IR difference spectra associated with these two phases. The results presented here provide support for the assignment made earlier, that the first photon absorption event creates changes in the protein structure only, and that only after continued illumination, Pchlride is converted into Chlide.

Combining the results from the femtosecond visible pump-probe and those in the mid-IR we conclude that absorption of the first photon activates the enzyme, which results in a high quantum yield formation of I675\* on the picosecond timescale when a second photon is absorbed. The structural changes are currently difficult to quantify by the spectroscopic changes in the mid-IR, and may involve minor structural rearrangements, optimising the alignment of the NADPH-nicotinamide ring and the tyrosine with the D ring of Pchlride to increase the rate of the hydride and proton transfers. On the other hand, the long lifetime (chapter 3) and the fact that activation is not reversed upon turnover of the enzyme (chapter 3) may suggest an irreversible process in the POR protein. It would appear that the conformational change is both highly efficient (i.e. it needs only one photon) and very specific, resulting in a high catalytic quantum yield.

The strong downshift of the keto  $13^1$  C=O stretching frequency in Pchlride bound to the enzyme is evidence for a strong H-bonding interaction between the keto group and protein residues. The upshift in the frequency of the coordination marker mode suggests a five-coordinated state of Pchlride in the enzyme active site, and consequently one coordination interaction between a protein residue, or a water molecule, and the Mg atom of Pchlride. We further conclude that the formation of the I675\* catalytic intermediate is associated in the mid-IR region with a decrease of the C=O keto oscillator strength.

A number of specific conserved POR residues were shown to be important for its catalytic activity and may be involved either in catalysis or in closer positioning of the Pchlride substrate to the NADPH cofactor upon activation<sup>(14, 81, 82)</sup>. The conserved Cys-307 residue is involved in binding of Pchlride, and Tyr-275 and Lys-279 are essential for catalytic activity. Certainly, in the future a more detailed insight into the events occurring in the POR enzyme can be achieved by performing similar FTIR difference absorption measurements in the regions of characteristic absorptions for these amino acids, and undoubtedly the exact determination of POR crystal structure will be important as well.

## 4.6. Appendix

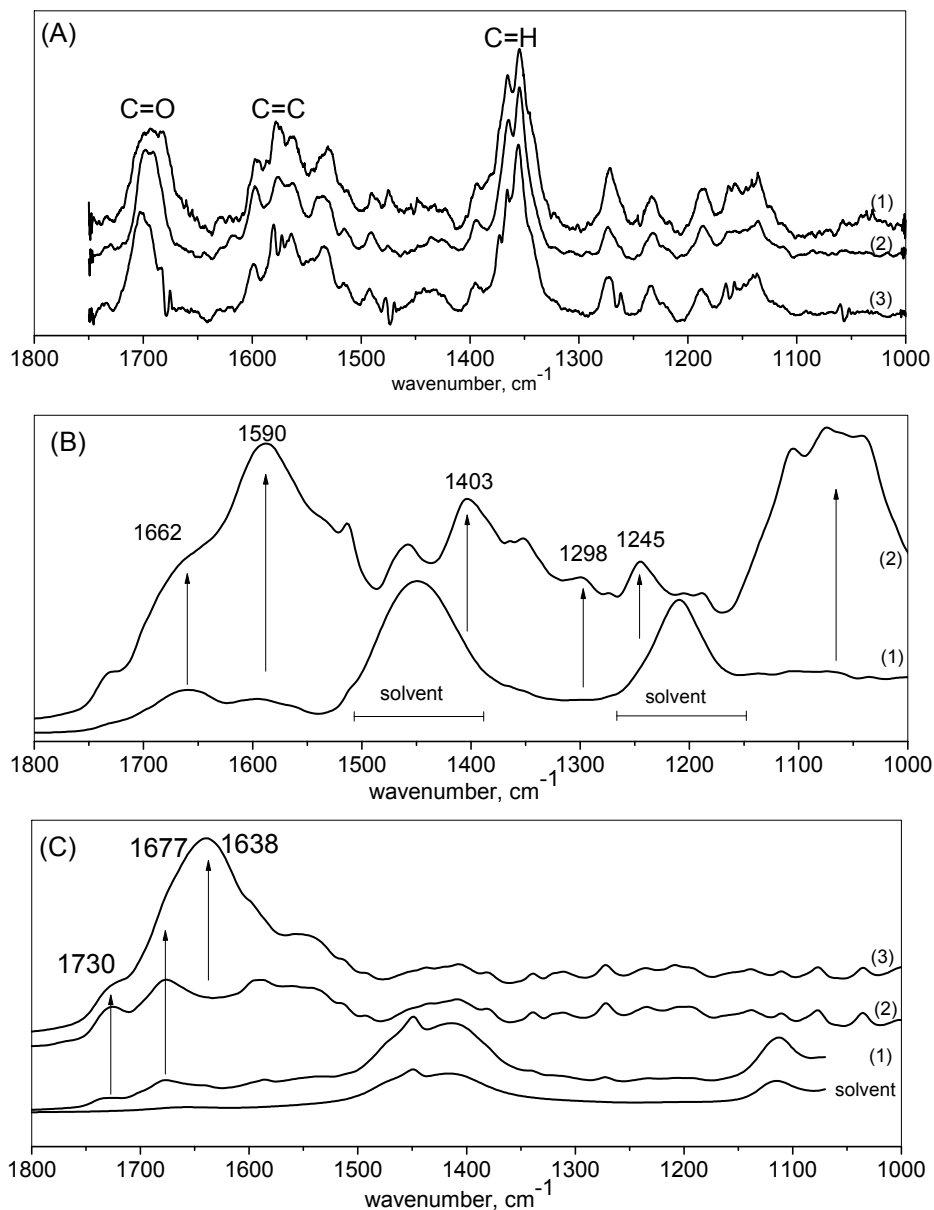


**Figure 4.6.** (A) Resonance Raman spectra of Pchlride, (1) methanol, (2) DMSO, (3) acetone. (B) ATR FTIR spectra of Pchlride in wet (1) and dry (2)  $\text{D}_2\text{O}$  buffer solution. (C) ATR FTIR spectra in wet (1,2) and dry (3) methanol. Arrows indicate the enhancement of specific bands upon solvent evaporation.

## **Resonance Raman Spectra of Protochlorophyllide in Solution**

In order to investigate the influence of the solvent environment on the position of keto and skeletal modes of Pchl<sub>id</sub>e, ATR FTIR (attenuated total reflection FTIR) and resonance Raman (RR) techniques were applied. Several solvents were used: D<sub>2</sub>O Tris/Triton buffer in the same composition as for POR experiments, methanol, DMSO, and acetone. RR spectra were recorded with spectral resolution of 1 cm<sup>-1</sup> using a U1000 double monochromator (Jobin Yvon, Longjumeau, France) equipped with an ultra-sensitive, deep-depleted, front illuminated CCD (Jobin Yvon). Excitations was provided by a Innova 90 Krypton laser with power of about 10 milliwatts at 441 nm.

In contrast to the IR active modes associated with changes in the permanent dipole detected by FTIR spectroscopy, Raman spectroscopy is able to detect modes that posses a change in polarizability, thus complementing the structural information about a polyatomic molecule.

The obtained resonance Raman spectra of Pchl<sub>id</sub>e upon 441 nm excitation in methanol, DMSO and acetone are shown in figure 4.6. A number of broad intense Raman signals are observed between 1700 cm<sup>-1</sup> and 1680 cm<sup>-1</sup> corresponding to the C=O keto modes, between 1600-1500 cm<sup>-1</sup> corresponding to the C=C skeletal vibrations, at 1400-1300 cm<sup>-1</sup> probably originating from the C-H stretching.

### **ATR FTIR spectra of Aggregated Pchl<sub>id</sub>e**

The ATR FTIR spectra of Pchl<sub>id</sub>e recorded in wet and dry D<sub>2</sub>O buffer and methanol are shown in figure 4.6.B, C. The droplet of the sample was placed on the sample window and the spectrum of wet solution was acquired, then the spectrum of dry pigment was recorded every minute. The clear broadening of some bands and dramatic enhancement of their intensity is observed upon solvent drying. The strong band in D<sub>2</sub>O buffer appears at 1586 cm<sup>-1</sup> (figure 4.6.B), together with significant gain in the intensity of bands at 1400 cm<sup>-1</sup> and around 1050 cm<sup>-1</sup>. In dry methanol (figure 4.6.C) the dominating band is at 1638 cm<sup>-1</sup> and perhaps hides in shoulders other signals. In both dry solvents specific bands become significantly enhanced and also additional ones below 1400 cm<sup>-1</sup> appear if compare to corresponding spectra in wet solvents. The observed spectral changes are likely to occur due to pigment aggregation upon solvent drying. A dense packing of molecules upon aggregation leads to strong  $\pi$ - $\pi$  coupling between adjacent molecules. The optical properties of Pchl<sub>id</sub>e aggregates in the visible region will be elaborated in chapter 6, 7.